www.vbripress.com/aml, DOI: 10.5185/amlett.2016.6499 Published online by the VBRI Press in 2016

Preparation and characterization of polyvinyl alcohol–pectin cryogels containing enrofloxacin and keratinase as potential transdermal delivery device

Jimena S. Gonzalez[1*], Yanina N. Martínez[2], Guillermo R.Castro[2], Vera A. Alvarez[1]

[1]*Grupo de Materiales Compuestos de Matriz Polimérica (CoMP)- Instituto de investigación en Ciencia y Tecnología de Materiales - INTEMA (CONICET-UNMdP), Solis 7575, (B7608FDQ) Mar del Plata (B7608FDQ), Argentina*
[2]*Laboratorio de Nanobiomateriales, CINDEFI - Departamento de Química, Facultad de Ciencias Exactas, Universidad Nacional de La Plata - CONICET (CCT La Plata), 1900, La Plata, Argentina*

[*]Corresponding author. Tel.: (+54223) 4816600 Ext 321 (Office); E-mail: jimena.gonzalez@fi.mdp.edu.ar

Received: 02 March 2016, Revised: 21 April 2016 and Accepted: 23 May 2016

ABSTRACT

Polyvinyl alcohol (PVA) and polyvinyl alcohol-pectin (PVA-P) cryogels are potential devices for wound healing. These materials have advantages over commercial wound dressings such as: retaining an appropriate level of moisture around wound and gas permeability and antibacterial properties. In a previous work, PVA-P cryogels containingan antibiotic and an enzyme (enrofloxacin and keratinase respectively) have been developed with promising results. In the present work, an exhaustive chemical, morphological and physical characterization of these films was carried out in order to explain the effect of incorporation of pectin into PVA matrix. The results show that the presence of pectin in PVA cryogel increase the size of PVA nanodomains determined by XRD patterns indicating an interaction between both PVA and pectin polymers. PVA nanodomains and crystallinity degree changed when enrofloxacin and keratinase were immobilized into PVA-P cryogels determined by SAXS and DSC analysis. These results suggest a good incorporation of both drugs into the polymeric matrix. A model involving the complex formation between the enzyme and enrofloxacin allocated through and between PVA nanodomains is proposed and it correlates well with results obtained in previous work where enrofloxacin kinetic release was found retarded by the presence of keratinase in the cryogels. Copyright © 2016 VBRI Press.

Keywords: PVA; pectin; enrofloxacin; keratinase; cryogel.

Introduction

Transdermal polymeric patches are low cost systems used to treat numerous non-communicable diseases (*e.g.* non-infectious and non-transmissible pathologies among people). For instance, nicotine and anticholinergic transdermal patches are now in the WHO model list, as necessary medicines for a basic care health system [**1**]. Nowadays second and third generation transdermal systems (for the delivery of macromolecules, vaccines and drugs avoiding gastrointestinal tract and high dose administration) are being studied using novel approaches [**2**]. Polyvinyl alcohol is a low cost, synthetic, biocompatible and FDA-approved polymer for the development of biomedical devices such as eye lenses, artificial tears and soft tissues replacements [**3, 4**]. PVA cryogel films, obtained by a simple and efficient method which consist in subsequent cycles of freezing and thawing of PVA aqueous solution, give rise to PVA crystals which are essentially packed by hydrogen bridges between PVA chains and they are likely responsible for the polymeric cross-linking. This structure has in consequence, a porous matrix where molecules can be allocated and also can diffuse along the film [**5**]. The structure of PVA cryogel is useful to track changes on the properties of the material related to changes in degree of crystallinity and in the size and distance of PVA nanodomains. Incorporation of macromolecules into the polymeric network may lead to the matrix rearrangements due to interaction with polymeric chains or by physical occlusion of the macromolecules into the nanometric domains [**6**]. In consequence, an understanding on the controlled release and polymer-biomolecule interactions can be explained by searching into PVA structure.

In a previous work, polyvinyl alcohol (PVA) - pectin (P) films doped with a keratinase (Ker) and enrofloxacin (Enro) was proposed for the treatment of eschars caused by burns and ulcers acting as a patch in the place of the injury with or without infection [**7**]. Pectin has a great effect on that behavior due to the interactions between them and Enro. A controlled release of both cargo molecules, Ker for necrotic tissue debridement and Enro for infection eradication, could be used as a beneficial alternative to surgery of necrotic tissue in burns and ulcers. A dependency on the concentration of pectin esterification

degrees and Ker release, which was related with the binding effect of Enro due to the hydrophobicity of pectins of large metoxiles, was observed. PVA-P doped with Ker and Enro were developed and sustained release was acquired. However, the Enro release kinetic was slower after the incorporation of keratinase to the matrix. A full characterization study of these materials and the influence of the drugs/enzyme on the matrix have not been reported until this work.

The aim of the present work was to characterize the PVA-P matrix by means of crystalline properties (e.g. XRD and SAXS) and thermo-analysis (Dynamic Scanning Calorimetry: DSC and Thermogravimetric Analysis: TGA) in order to correlate structural properties with the behavior of PVA-P films containing Ker and Enro.

Experimental

Materials / chemicals details

PVA (M_W13–23 KDa, 98–99% hydrolyzed) was purchased from Sigma-Aldrich (United States of America). Pectin with a 55.0 % of esterification degree was kindly supplied by CPKelco (Buenos Aires, Argentina). Ker and Enro were supplied by Sigma-Aldrich (United States of America). All remaining reagents were from analytical grade or similar quality.

Preparation of aqueous solution polymers

Stock solutions of 30% (w/v) PVA were prepared in distilled water. The mixture was heated at 80°C for 90 minutes with slow stirring until total dissolution. Solutions of 2.00% to 4.00% (w/v) pectin were prepared in distilled water with slow stirring.

Preparation of cryogel film, enrofloxacin and enzyme immobilization

Aqueous stock solutions of 30.0% (w/v) PVA were mixed with 2.00%–4.00% (w/v) pectin and properly diluted to obtain 15.00/1.00, 15.00/0.75 and 15.00/0.50% (w/w) PVA/pectin solutions. Then, 1.0 enzyme units (EU) of keratinase and 5.0 µg/ml of enrofloxacin were added to the gels. Each solution was cast into Petri plates, frozen at −18 °C for 20 h and then thawed at room temperature (25 °C) for 8 h. This cycle of freezing/thawing was repeated three times.

Small angle X- ray scattering (SAXS)

SAXS measurements were carried out with an incident beam of 8 KeV and λ= 1.55 Å at D1B-SAXS1 beam-line using a Pilatus 3000K detector (National Laboratory of Synchrotron Light, Campinas, Brazil). Solid samples were placed into stainless steel sample holder and holded in both sides using Kapton tape. All samples were measured at room temperature. Silver behenate powder was used to calibrate the distance among samples, detector and beam direction. Samples were measured in a distance of 0.8 m between sample and detector.

X- ray diffraction (XRD)

Dried sample diffraction patterns were collected at room temperature with an analytical expert instrument using K_∞Cu radiation (λ=1.54 Å) and scans at 2 º/minute in the 2θ range 3-60º. The generator tension was 40 kV and current of 40 mA.

Fourier transformed infrared spectroscopy (FTIR)

FTIR spectra of samples were obtained in a Thermo Scientific Nicolet 6700 spectrometer, with a resolution of 4 cm^{-1}. 32 scans were performed over each sample from 600 to 4000 cm^{-1}, the ATR (Attenuated Total Reflectance) accessory was utilized to perform the measurements.

Differential scanning calorimetry (DSC)

Measurements were carried out in a TA-Instrument (model Q2000 V24.10 Build 122; New Castle, DE, USA). Samples were scanned from 20 to 250 °C at a heating rate of 10 °C/min, under nitrogen atmosphere. The melting temperature (T_m) was determined from the obtained curve and the degree of crystallinity (X_{cr}, %) was calculated.

Thermogravimetric analysis (TGA)

Thermogravimetric studies were carried out in a Universal V4.5A TA Instruments (New Castle, DE, USA). All samples were scanned from room temperature to 600 °C at 10 °C/min under nitrogen atmosphere. The bound water content (*BW, %*) and degradation temperature (*Tp*) was obtained from the TG curves.

Scanning electron microscopy (SEM)

Samples were firstly swollen, frozen, lyophilized and then cryofractured with N2 liquid and coated with gold before testing. After that, the surface was sputtered with gold using a metalizer (Balzers SCD 030), obtaining a layer thickness between 15 and 20 nm. Film surfaces and morphologies were observed by SEM (Philips SEM 505 model, Rochester, NY, USA).

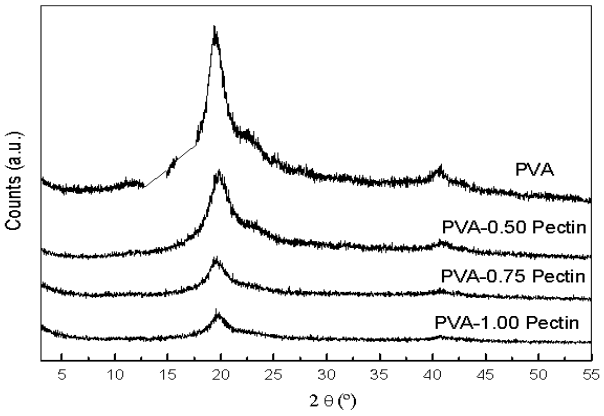

Fig. 1. X-ray diffraction patterns of PVA with different concentrations of Pectin 55 (%, w/v).

Results and discussion

Structure of PVA- pectin blend

The X-ray diffraction spectra showed two characteristic peaks centered at 19° and 22° (2θ values) assigned to semicrystalline PVA and corresponds to (1 0 1) and (1 0 $\bar{1}$)

reflection planes, respectively (**Fig. 1**) [**8, 9**]. XRD diffraction is giving relevant information about the periodic arrangements of the material. The peak 101 intensity reflection of PVA is decreasing with the increase of P55 concentration into the cryogel (**Fig. 1**). The 101 reflection denotes intermolecular hydrogen bonding interaction among PVA chains [**10**]. As the intensity of the intermolecular H- bonding interaction decreases, it is possible that new hydrogen bridges are established between PVA and P55. It was reported before that pectin and PVA polymeric chains interact via H- bonded forces when composites were synthesized [**11**]. Assuming that PVA nanodomains (also named as nanocrystals) can be considered as nanospheres included into a polymeric matrix, information on their size can be obtained by using a physical approach. The size of nanospheres can be measured by the Scherrer's equation which provides information on size changes by addition of another polymeric material [**12**]. As it is shown in **Table 1**, the size of PVA nanodomains (L, in nm, by Scherrer's equation) increased more than twice by increasing pectin concentration at 1.00% (w/v). The results suggest that during nanocrystals formation in presence of pectin after the freezing and thawing cycles, the pectin chains intercalate between PVA chains probably interacting by Hydrogen bonds. As a consequence, the size of the resulting nanocrystal in the composites became bigger.

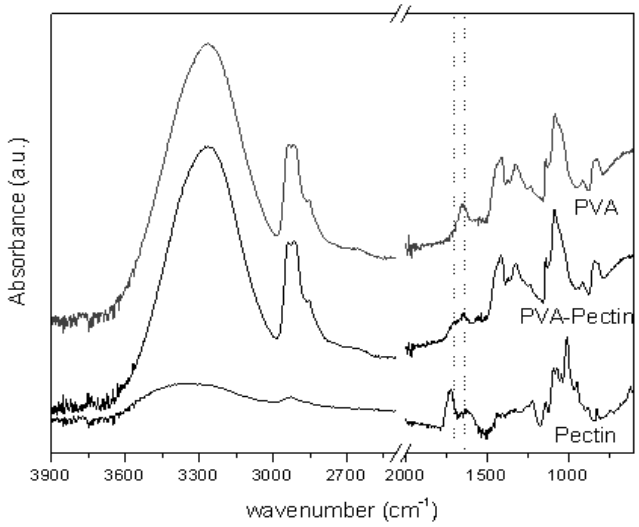

Fig. 2. FTIR spectra of PVA and PVA-Pectin hydrogels.

In **Fig. 2** are shown the FTIR spectra of pectin, PVA hydrogel and PVA-0.5 pectin hydrogel, from this, it is possible to observe the characteristic peaks of pectin, the free carboxyl group and the esterified group, typically they appear at 1650 and 1750 cm^{-1} respectively [**13**], however in our hydrogel these peaks are slightly shifted into a lower wavelength (1642 and 1705 cm^{-1}) suggesting an interaction between both polymers. DSC studies were carried out to confirm the hypothesis of PVA-pectin interactions. As mentioned before, semi crystalline characteristics of PVA are useful to monitor changes in the nanocrystal domains of the matrix. As shown in **Fig. 3**, there are two endothermic peaks corresponding to the melting of pectin and PVA nanostructures (**Table 1**). The melting temperature (T_m) of the pectin crystals varies from 168.2 to 176.3 °C according to the literature [**14**] and the ΔH of the pectin increases with the pectin content in the hydrogel as we expect. The Tm of the PVA crystals does not show significant changes, however the crystallinity degree decreases with the incorporation of pectin indicating a reduction of the crystalline order of the PVA due to the presence of pectin. It well known that the physical properties of polymer blends strongly depend on their crystallization behavior and morphology. In a two component polymer blend, if the crystallization temperature of one component is higher than that of the other component, then the former crystallizes in the presence of the molten state of the other component whereas the second component crystallizes in the presence of the solidified phase of the first component [**15**]. The presence of a second component either in the molten or solid state affects both the nucleation and crystal growth of the crystallizing polymer.

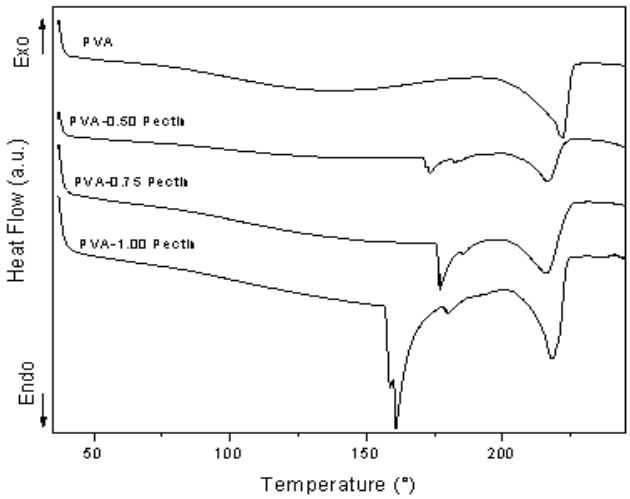

Fig. 3. DSC measurements of the PVA cryogels with different amounts of pectin 55 (%, w/v).

Table 1. Main properties of PVA samples with different concentrations of pectin 55 (%, w/v).

Pectin (%, w/v) content on PVA samples	DRX L (nm)	DSC				TGA	
		T_{m1} (ºC)	Pectin ΔH (J/g)	T_{m2} (ºC)	PVA X_{cr} (%)	P_I (ºC)	P_{II} (ºC)
0.00	1.74	-	-	222.1	37.5	143.1	281.9
0.50	2.65	173.4	11.2	216.8	26.1	176.9	273.4
0.75	3.60	176.3	18.3	219.5	24.8	210.2	280.7
1.00	4.02	168.2	30.0	220.0	30	166.2	278.0
100 .00	-	-	-	-	-	57.9	243.9

The thermal analysis, in combination with other chemical and physical analytical means, is a suitable method for the investigation of the properties of PVA-pectin compounds. **Fig. 4** show the TGA and DTGA curves of PVA matrix and PVA-P composites where thermal degradations steps can be observed and the temperatures values are summarized in table 1. In the neat PVA hydrogel, the first step appears at 155.5 ºC which corresponds to the humidity loss, the second one at 281.9 ºC where a higher amount of mass is loss, corresponds to the detachment of lateral groups forming water, acetic acid and acetaldehyde as sub-

products. Finally, the last step, centered at 436.4 ºC, is in agreement with the total degradation of the polymer and the breaking of the polymeric chains [**16, 17**]. The pectin degradation was observed in one single peak at the temperature of 243.9 °C in accordance with [**18**], they have been reported for other pectins. In our pectin curve also appear a first peak in 57.9 °C corresponds to water loss. In the composites, the first step is in the range of 166-210 °C which correspond to a humidity loss from the PVA and an early degradation of pectin, showing a good interaction between both components.

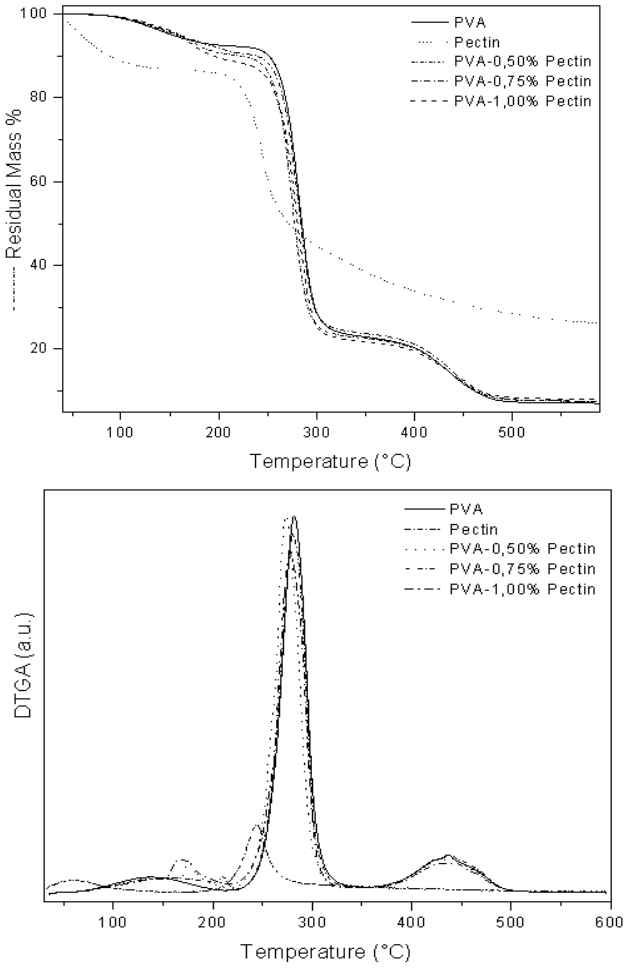

Fig. 4. (a) TGA and (b) DTGA analysis of PVA with different pectin 55 concentrations (%, w/v).

As previously shown, after XRD patterns analysis, a possible interaction between PVA and pectin 55 was observed. Also, DSC measurements showed a decrease on PVA crystallinity in presence of pectin. Hence, after pectin–PVA interactions were elucidated, it is important to get information on PVA-P properties after incorporation of Ker and Enro which matrix was developed in our previous work [**7**].

For the all obtained results it can be done a schematic representation of PVA films is shown in **Fig. 5**. Moreover, SEM images of PVA and pectin composites are clearly showing a markedly decrease in porous size with the incorporation of pectin.

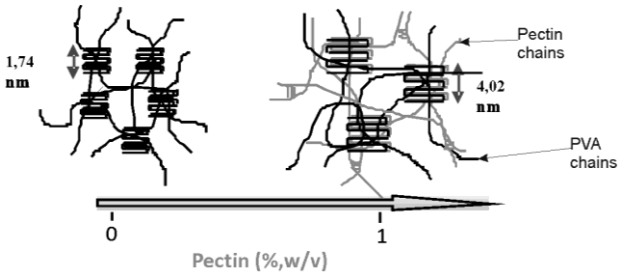

Fig. 5. Schematic representation of PVA nanodomains increased size by the presence of pectin.

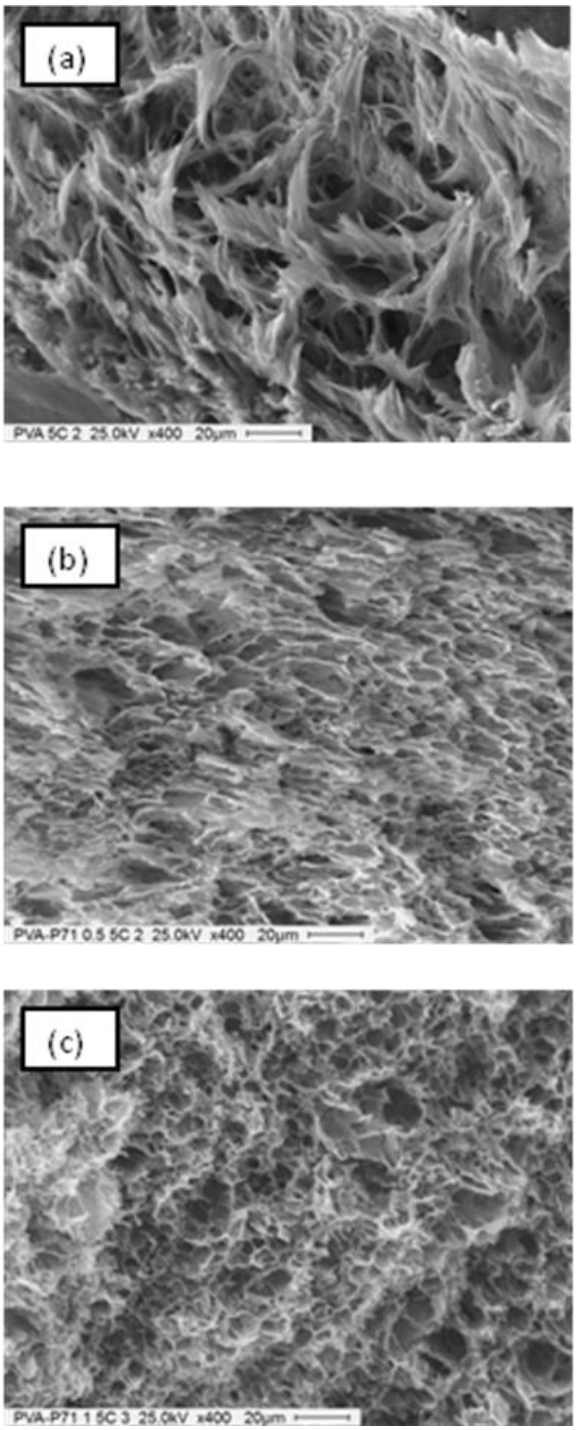

Fig. 6. Micrographs of a) PVA, b) PVA/0.5Pectin and c) PVA/1.0Pectin.

Structure of PVA pectin blend after the incorporation of ker and enro

SAXS studies were performed in order to obtain information on the nanostructure of PVA and the consequent changes after the incorporation of pectin, Enro and Ker into the polymeric PVA and PVA-P nanostructure networks. In this case, the pectin concentration in all the samples was 0.50% (w/v) because it was the concentration needed to obtain a faster release of Enro from the PVA-P matrix, as shown in our previous work. Henceforth, the pectin concentration was fixed to 0.50% (w/v) in all the studies developed. The values of the maximum on q vector intensity (qmax) were obtained from the SAXS patterns in all the samples as seen in **Fig. 7**.

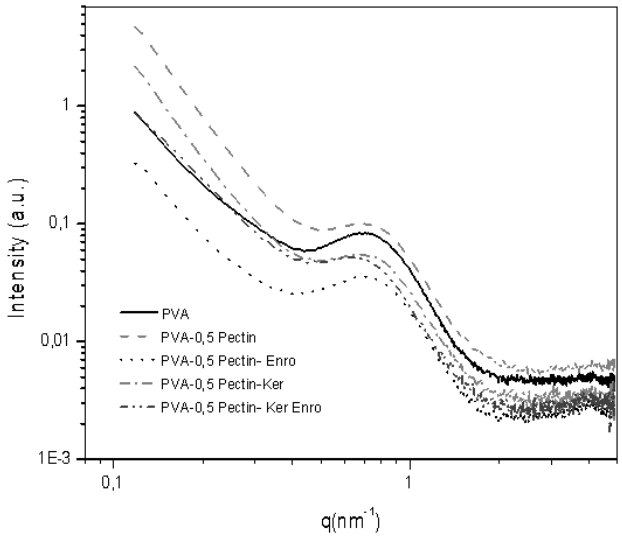

Fig. 7. SAXS patterns of PVA samples without and with pectin 55 (0.50 %, w/v), enrofloxacin and/or keratinase.

It was observed that in presence of pectin-Enro-Ker the $q_{max} = 0.64$ nm^{-1}. However, the q_{max} was 0.7 nm^{-1} in PVA samples with or without pectin. The shift in q_{max} denotes the incorporation of both components keratinase and enrofloxacin into the nanodomains of PVA-P. As seen in **Table 2** and by assuming the nanocrystals of PVA as spheres embedded into the polymeric network it was possible to calculate de distance between PVA and PVA-P nanodomains which was d= 8.97 nm in both cases. After the incorporation of keratinase, the distance increased to 9.01 nm and when both components Ker and Enro were incorporated into PVA-P matrix the distance increased to 9.98 nm. These results imply the incorporation of both components between PVA-P nanodomains because of the distance increased 1 nm. On the other hand, an increased into PVA-P nanodomains size due to the incorporation of Ker and Enro is denoted.

Calorimetric measurements showed an increase in the crystalline degree (X_{cr}) of PVA in the presence of pectin-enrofloxacin-keratinase (**Table 2** and **Fig. 8**). These results are confirming the SAXS measurements where a possible location of keratinase-complex was proposed into PVA-P nanodomains (**Fig. 9**). As the distance of PVA-P nanodomains changed it is possible to expect a change in the crystalline properties because the size of PVA-P. A model of a complex between Enro and Ker formation is proposed because after the incorporation of the molecules in separate, no such increase in the distance of PVA-P nanodomains was observed (**Fig. 9**). As it was reported previously, Enro is able to bind proteins in a 40% to plasma involved in the clearance of drugs [**19**]. These results may explain the complex formation between Enro and Ker.

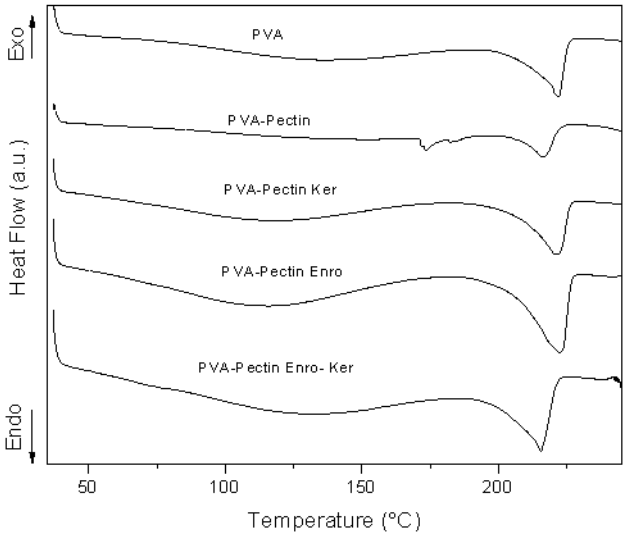

Fig. 8. DSC curves of PVA, PVA-0.5 Pectin and PVA-0.5 Pectin with enrofloxacin and keratinase.

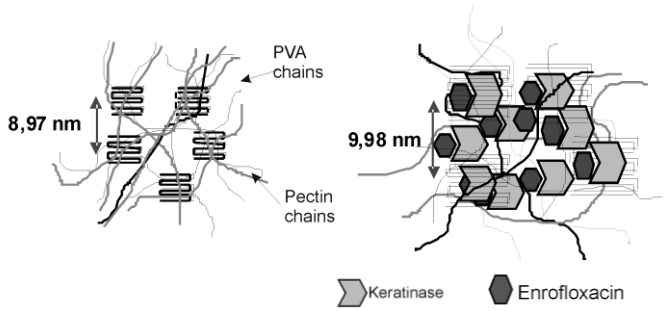

Fig. 9. Schematic illustration of PVA-P network affected by the incorporation of enrofloxacin and keratinase.

Table 2. DSC and SAXS results for PVA-0.5%Pectin films.

PVA samples supplemented with	DSC		SAXS	
	T_m (ºC)	Xcr (%)	q (nm^{-1})	d (nm)
None	222.1	37.5	0.70	8.97
0.5% Pectin	216.8	26.1	0.70	8.97
0.5% Pectin -Enrofloxacin	222.2	51.2	0.70	8.97
0.5% Pectin - keratinase	220.4	51.3	0.69	9.01
0.5% Pectin -Enro-keratinase	215.5	35.1	0.64	9.98

Conclusion

The analysis of the PVA-P matrix characterized by XRD and DSC studies suggests an interaction of PVA and pectin. Also, pectin chains intercalate between PVA polymeric chains to form bigger nanocrystals affecting its crystalline properties which is correlated with a decrease of 11.4 % in the degree of PVA crystallinity. After the incorporation of keratinase and enrofloxacin into PVA-P matrix, SAXS

measurements showed an increased in about 1 nm on the distance between PVA-P and PVA nanodomains. These results suggest the incorporation of a complexed form of keratinase and enrofloxacin into the polymeric nanodomains. In previous work, a slower release kinetic of enrofloxacin was observed in presence of keratinase in comparison with enrofloxacin alone. SAXS results may help to understand this phenomenon where the formation of a complex between enrofloxacin and keratinase allocated through the polymeric nanodomains may be the causative of such decrease in enrofloxacin release kinetic. In this way, enrofloxacin molecules are bound to the enzyme so a sized restriction release from the polymeric matrix is proposed.

Finally, the structural characterization of enrofloxacin and keratinase into the PVA-P films determined in the present work allows for criteria to change the composition associated to the cargo release from the gels based on the requirements for the treatment of wounds and eschars to be applied as patches in the microbial infected dermal zones.

Acknowledgements

The present work was supported by Argentinian grants from CONICET (National Council for Science and Technology, PIP 0214), The National Agency of Scientific and Technological Promotion (ANPCyT), UNLP (National University of La Plata, 11/X545) and UNMdP (National University of Mar del Plata). We want to thank Dr. Mateus Cardoso (National Laboratory of Synchrotron Light, Campinas, Brazil) and to Ms. Fiona M. Britto for the synchrotron SAXS measurements.

Reference

1. WHO Model List of Essential Medicines (**2013**). http://www.who.int/medicines/publications/essentialmedicines/en/
2. Kataria, K.; Gupta, A.; Rath, G.; Mathur, R.B.; Dhakate, S.R.; *Int J Pharm* **2014**, 469,1,102-110. **DOI:** 10.1016/j.ijpharm.2014.04.047
3. Gonzalez, J.S.; Alvarez, V.A.; *J Mech Behav Biomed Mat* **2014**, 34, 47-56. **DOI:** 10.1016/j.jmbbm.2014.01.019
4. Campoccia, D; Montanaro, L.; Arciola, C.; *Biomaterials* **2013**, 34, 8533–8554. **DOI:** 10.1016/j.biomaterials.2013.07.089
5. Hassan, C.M. and Peppas, N.A.; *Adv Polym Scie* **2000**, 153,37-36 **DOI:** 10.1007/3-540-46414-X_2
6. Mansur, H.S.; Mansur, A.A.P.; Oréfice R.L.; *Solid State Phenom* 12, 1355-1358. **DOI:** 10.4028/www.scientific.net/SSP.121-123.1355
7. Martínez, Y. N., Cavello, I., Hours, R., Cavalitto, S., and Castro, G. R., *Bioresour Technol* **2013**, 145: 280-284 **DOI:** 10.1016/j.biortech.2013.02.063
8. Ricciardi, R., Auriemma, F., Gaillet, C., De Rosa, C., and Lauprêtre, F., *Macromol* **2004**, 37: 9510-9516. **DOI:** 10.1021/ma048418v
9. Gupta, S., Pramanik, A. K., Kailath, A., Mishra, T., Guha, A., Nayar, S., & Sinha, A, *Colloids Surf B* **2009**, 74, 186-190. **DOI:** 10.1016/j.colsurfb.2009.07.015
10. PO-DA HONG, J. H. C., & WU, H. L.; *J Appl Polym Sci* **1998**, 69, 2477-2486. **DOI:** 10.1002/ (SICI) 1097-4628 (19980919) 69:12 < 2477:: AID-APP19>3.0.CO;2-U
11. Latif IA, Abbas SM, Kadhum MA, *Chem Mater Res* **2013**, 3, 1-13.
12. Cullity Berrard D; Elements of X-ray diffraction, *Ed. Biblio Bazaar*, 3rd edn; **2001**.
13. Gnanasambandam, R.; Proctor, A.; *Food Chemistry*. **2000**, 68, 3, 327-332. **DOI:** 10.1016/S0308-8146(99)00191-0
14. Singthong J., Cui S.W., Ningsanond S., Douglas Goff H., *Carbohydrate Polymers*. **2004**, 58, 4, 391–400. **DOI:** 10.1016/j.carbpol.2004.07.018
15. Huang JW, Wen YL, Kang CC, Yeh MY, Wen SB., *Termochim Acta* **2007**, 465, 48-58. **DOI:** 10.1016/j.tca.2007.09.004
16. Barrera, J.E.; Rodriguez, J.A.; Perilla, J.E. and Algecira, N.A., *Rev Ing Inv* **2007**, 27, 100-105.
17. Zheng, Pe.; Ling X. K., *Polymer Degradation and Stability* **2007**, 92, 1061e1071.
18. Einhorn U., Stoll, H.K., Dongowski G., *Food Hydrocolloids*, **2007**, 21, 7, 1101–1112. **DOI:** 10.1016/j.foodhyd.2006.08.004
19. Zlotos G; Protein binding in a congeneric series of antibacterial quinolone derivatives, *J Pharm Sci* **1998**, 87, 215-220. **DOI:** 10.1016/S0378-5173(98)00126-4
20. Peppas N.A. and Merrill E.W., *J Appl Polym Sci* **1976**, 20, 1457-1465. **DOI:** 10.1002/app.1976.070200604

Supporting information

(a) Chemical formulas/ theoretical calculations

Scattering vector (q) was analyzed versus intensity as following equation,

$$q = (4\pi /\lambda) \text{ sen}\theta \quad (1)$$

where, 2θ is the dispersion angle.

Assuming the model of PVA nanocrystals as spheres embedded in a polymeric matrix, the average distance (d) between PVA nanocrystals can be estimated under the following equation,

$$d = 2\pi/qmax \quad (2)$$

where, qmax is the modulus of the scattering vector corresponding to the maximum of the SAXS intensity function.

The size of PVA nanocrystals can be estimated by using Scherrer equation [**12**],

$$L= (K . \lambda)/(\beta . \cos\theta) \quad (3)$$

where k = 1 assuming that PVA nanocystals are spherical, β is the width at half maximum intensity of the reflection, θ is Bragg's angle and λ=1.54 Å is the wavelength of the X-ray radiation.

The degree of crystallinity (Xcr, %) was calculated from the following equation,

$$Xcr (\%) = \Delta Hm/(\Delta H°m(1-mf)) \times 100 \quad (4)$$

where, ΔHm was determined by integrating the area under the melting peak over the range of 190-240 °C, ΔH°m was the heat required for melting a 100% crystalline PVA sample (138.6 J/g) [**20**] and mf is the mass fraction of pectin.